6. I. W. J. Still and J. R. Strautmanis, *Tetrahedron Lett.*, **30**, 1041 (1989).
7. (a) P. H. H. Hermkens, J. H. V. Maarseveen, C. G. Kruse, and H. W. Scheeren, *Tetrahedron Lett.*, **30**, 5009 (1989); (b) P. H. H. Hermkens, J. H. V. Maarseveen, H. W. Berens, J. M. M. Smits, C. G. Kruse, and H. W. Scheeren, *J. Org. Chem.*, **55**, 2200 (1990).
8. B. H. Yoon, H. S. Lyu, J. H. Hahn, and C. M. Ahn, *Bull. Korean Chem. Soc.*, **12**, 380 (1991).
9. D. R. Hwang, P. Helquist, and M. S. Shekhani, *J. Org. Chem.*, **50**, 1264 (1985).
10. (a) K. Oki, K. Suzuki, S. Tuchida, T. Saito, and H. Katake, *Bull. Chem. Soc. Jpn.*, **43**, 2554 (1970); (b) C. H. Wong and K. T. Wang, *Tetrahedron Lett.*, **19**, 3813 (1978).
11. Th. J. de Boer and H. J. Backer, "*Organic Syntheses*" (Wiley, New York, 1963), Col. Vol. IV, pp. 250.
12. (a) A. Ito, R. Takahashi, and Y. Bara, *Chem. Pharm. Bull.*, **23**, 3081 (1975); (b) L. I. Zarharkin and I. M. Khorlina, *Tetrahedron Lett.*, **14**, 619 (1962).
13. S. Akabori, S. Sakakibara, Y. Shimonishi, and Y. Nobuhara, *Bull. Chem. Soc. Jpn.*, **37**, 433 (1964).
14. G. F. Smith, *J. Chem. Soc.*, 3842 (1954).
15. (a) B. T. Ho, W. M. Mclsaac, and L. W. Tansey, *J. Pharm Sci.*, **58**, 563 (1969); (b) E. H. P. Young, *J. Chem. Soc.*, 3493 (1958).
16. R. S. Varma and G. W. Kabalka, *Synth. Commun.*, **15**, 151 (1985).
17. (a) E. J. Corey and H. Estreicher, *J. Am. Chem. Soc.*, **100**, 6294 (1978); (b) K. Oliver, "*Organic Synthesis*" (Wiley, New York, 1941), Coll. Vol. 1, pp. 445.
18. (a) H. C. J. Ottenheijm, R. Plate, J. H. Noordick, and J. D. M. Herscheid, *J. Org. Chem.*, **47**, 2147 (1982); (b) T. L. Gilchrist, D. A. Lingham, and T. G. Roberts, *J. Chem. Soc., Chem. Commun.*, 1089 (1979).
19. (a) T. L. Gilchrist and T. G. Roberts, *J. Chem. Soc., Perkin Trans. 1.*, 1283 (1983); (b) J. Ratusky and F. Sorm, *Chem. Listy.*, **51**, 1091 (1957).
20. (a) R. Plate, P. H. H. Hermkens, J. M. M. Smits, and H. C. J. Ottenheijm, *J. Org. Chem.*, **51**, 309 (1986); (b) Y. Kigukawa and M. Kawase, *Chem. Letters*, 1279 (1977).
21. C. Salvator, M. Antonio, and S. Mario, *Synthesis*, 799 (1976).
22. D. Theodoroponlos, *Acta Chem. Scand.*, **13**, 383 (1976).
23. G. Cavallini, V. Ravenna, *Il Farmaco (Pavia) Ed. Sci.*, **13**, 113 (1958); *Chem. Abstr.*, **52**, 20126i (1958).

NMR Relaxation Study of Segmental Motions in Polymer-*n*-Alkanes

Jeong Yong Chung, Jo Woong Lee*, Hyungsuk Pak, and Taihyun Chang†

Department of Chemistry, College of Natural Sciences Seoul National University, Seoul 151-742
†Department of Chemistry, Pohang Institute of Science and Technology, Pohang 790-600
Received January 16, 1992

^{13}C spin-lattice relaxation times were measured for *n*-alkanes of moderate chain length, ranging from *n*-octane to *n*-dodecane, under the condition of proton broad-band decoupling within the temperature range of 248-318 K in order to gain some insight into basic features of segmental motions occurring in long chain ploymeric molecules. The NOE data showed that except for methyl carbon-13 dipole-dipole interactions between ^{13}C and directly bonded ^{1}H provide the major relaxation pathway, and we have analyzed the observed T_1 data on the basis of the internal rotational diffusion theory by Wallach and the conformational jump theory by London and Avitabile. The results show that the internal rotational diffusion constants about C-C bonds in the alkane backbone are all within the range of 10^{9}-10^{10} sec^{-1} in magnitude while the mean lifetimes for rotational isomers are all of the order of 10^{-11}-10^{-10} sec. Analysis by the L-A theory predicts that activation energies for conformational interconversion between *gauche* and *trans* form gradually increase as we move from the chain end toward the central C-C bond and they are within the range of 2-4 kcal/mol for all the compounds investigated.

Introduction

Elucidation of motional behaviors of relatively short chain molecules such as *n*-alkanes of moderate chain length in neat liquid or dissolved state has eagerly been pursued by molecular scientists because it provides the basis of understanding of local segmental motions in more complex polymer molecules including biopolymers as well as synthetic ones. Despite great efforts by many investigators, however, fluxional nature of the structures of these chain molecules has thus far defied our attempts to describe their motional behaviors quantitatively in terms of simple dynamical models. The motions of each segment in these molecules are not fully independent of those of other segments in contrast to the case of small molecules. Instead, they are cooperatively coupled to one another in a complicated manner as is manifested by kink formation and propagation.[1-3] In order to make the analysis of these complicated motions mathematically tractable one usually treat the problem as that of multiple internal rotations about the skeleton σ bonds, which in-

volve rapid interconversion among various rotational isomers, and ignore all other modes of bond stretching and deforming vibration. Even with this simplifying approximation it still remains formidable to treat the problem quantitatively since internal rotation about a single bond may induce complicated cooperative counter-rotations about neighboring bonds due to the frictional forces exerted by surrounding solvent molecules.

Although dynamical motions of a wormlike chain can be kept track of as a function of time under some given conditions using the powerful modern computer techniques,[4-8] it is also desirable to find a simple model which can provide a qualitative and intuitive description of those modes of motions which make predominant contributions to the relaxation mechanism of interest. The brute-fore computer techniques can provide detailed dynamical informations about this system but their computational procedures, though fast and powerful, have some drawbacks in that they involve too many adjustable parameters and are time-consuming. Moreover, they are largely uneconomical when only qualitative treatment of data is required. For this reason we have attempted in this paper to interpret the observed relaxation time data for *n*-alkanes on the basis of internal rotational diffusion model such as treated by Wallach[9] (hereafter, referred to as the IRD model) and the London-Avitabile (L-A) model.[3] These two models are conceptually very crude and introduce some simplifying approximations to make the calculation manageable; nevertheless, they provide us a clearcut picture and, at least, a qualitative insight of the dynamical processes occurring in these molecules. Theory by Monnerie *et al.*[10,11] provides more sophisticated, quantitative explanation of these processes, but we have adopted more naive models, particularly the L-A model, in the hope that they might serve as a stepping stone for a more refined theory that we intend to develop along the similar line in the near future.

In the present study several branchless *n*-alkanes ranging from *n*-octane to *n*-dodecane have been dissolved in $CDCl_3$ and the spin-lattice relaxation time T_1 has been measured for each backbone carbon-13 in these compounds as a function of temperature under the condition of broadband proton decoupling. Thus obtained data have been interpreted on the basis of the IRD and the L-A model assuming that predominant relaxation mechanism is that due to dipolar couplings between directly bonded ^{13}C and ^{1}H. The results show that the rotational diffusion constants for carbons in the alkane backbone are all within the range of 10^9-10^{10} sec^{-1} in magnitude while the mean lifetimes for rotational isomers are on the average of the order of 10^{-10}-10^{-11} sec over the temperature range of 248-318 K. It is also confirmed that as we move along the carbon backbone from the center of chain toward terminal side T_1 value increases, indicating the chain end is more mobile than the center part. Activation energies for conformational interconversion between gauche and trans forms are found to be within the range of 2-4 kcal/mol for all the compounds investigated, which indicates that the conformational interconversions in these molecules probably proceed through type 2 transition as proposed by Helfand.[1,2]

Theory

It is well known that, if magnetic dipole-dipole interaction between ^{13}C and ^{1}H provides the dominant relaxation pathway, the spin-lattice relaxation time T_1 for a ^{13}C nucleus under broadband proton decoupling can be expressed as follows:[12]

$$\frac{1}{T_1}=\frac{N_H}{20}(2\pi R)^2[J_0(\omega_H-\omega_C)+3J_1(\omega_C)+6J_2(\omega_H+\omega_C)] \quad (1)$$

where R is the dipolar coupling constant defined by Eq. (2) and N_H is the number of protons attached to this carbon.

$$R=\left(\frac{\mu_0}{4\pi}\right)\gamma_H\gamma_C\frac{\hbar}{2\pi}r_{C\text{-}H}^{-3} \quad (2)$$

μ_0: magnetic permeability constant;
γ_H, γ_C: magnetogyric ratio of ^{1}H and ^{13}C, respectively;
$r_{C\text{-}H}$: distance between directly bonded ^{1}H and ^{13}C.

$J_m(\omega)$ is the spectral density at frequency ω of the relevant autocorrelation function $G_m(\tau)$ appearing in dipolar relaxation theory as shown in Eqs. (3) and (4):

$$J_m(\omega)=\int_{-\infty}^{\infty}G_m(\tau)\exp(-i\omega\tau)\,d\tau = 2\int_0^{\infty}G_m(\tau)\cos(\omega\tau)\,d\tau \quad (3)$$

and

$$G_m(\tau)=\langle Y_{2m}(\Omega_{C\text{-}H}(t))\,Y_{2m}^*(\Omega_{C\text{-}H}(t+\tau))\rangle, \quad (4)$$

where $Y_{2m}(\Omega_{C\text{-}H}(t))$ is the mth component of second-order spherical harmonics of the orientation of C-H internuclear vector, $\Omega_{C\text{-}H}(t)$, with respect to the laboratory fixed frame at time t and the angular bracket $\langle\ \rangle$ denotes the average over equilibrium ensemble. If the motion of C-H vector with respect to the laboratory-fixed coordinates is isotropic, then it can be shown that $G_m(\tau)$, hence $J_m(\omega)$, is independent of the index m. Therefore we will henceforth drop the index from the expressions for $G(\tau)$ and $J(\omega)$. Instead we will affix the subscript N to indicate the expressions are for the N-th carbon.

In order to study the segmental motions it is desirable to describe the relative motions of a C-H internuclear vector with respect to neighboring C-H vectors. Hence it would be convenient if we choose a molecule-fixed coordiantes frame whose origin is taken at the position of innermost carbon in the chain due to experimental considerations and then perform the transformation successively from this coordinates to the C-H bond-fixed coordinates through internal rotational coordinate transformations. If these transformations are invoked and use is made of the properties of Wigner rotation matrices associated with them, $G_N(\tau)$ can be shown to take the following form:

$$G_N(\tau)=\sum_{\substack{a,b,c\cdots,n\\ b',c'\cdots,n'}} d_{ab}(\beta)\,d_{ab'}(\beta)\cdots d_{n0}(\beta')\,d_{n'0}(\beta')$$
$$\times\exp(-6D_0\tau)\langle\exp[i\{a\gamma_0(0\to1)-a\gamma_\tau(0\to1)\}]\cdots$$
$$\times\exp[i\{n\gamma_0(N-1\to N)-n'\gamma_\tau(N-1\to N)\}]\rangle, \quad (5)$$

where N denotes the *N-th* carbon atom (counting from the innermost atom), the $(i-1)\to i$ symbol indicates the internal

coordinates system transformation, β is the polar angle between two successive C-C bonds, β′ is the azimuthal angle between C-C bond and successive C-H bond, and $d^{(2)}_{mm'}(\beta)$ is the real reduced Wigner matrix elements. We will assume here that the rotational motion of moleculefixed coordinates can be described by isotropic rotational diffusion constant D_0.

Calculation of the ensemble average in Eq. (5) has been attempted by several authors on the basis of various theoretical models such as internal rotational diffusion model,[9,13] jump diffusion model,[14,15] extended diffusion model,[16] etc. Among these we will restrict our attention to the IRD model used by Wallach and the L-A model proposed by London and Avitabile (a jump diffusion model) which we utilize to analyze our experimental results.

Internal Rotational Diffusion Model[9]. In this model it is assumed that the internal rotation about each C-C bond is free and independent of the rotation about other C-C bonds. The ensemble average in Eq. (5) may be calculate as follows:

$$<\exp[i(m\gamma_0-m'\gamma_\tau)]>$$

$$=\int\int d\gamma_0\, d\gamma_\tau\, P(\gamma_0,\ 0)\, P(\gamma_\tau,\ \tau|\gamma_0,\ 0)\exp[i(m\gamma_0-m'\gamma_\tau)] \tag{6}$$

where $P(\gamma_0, 0)$ is the orientational a priori probability of dihedral angle γ_0 at initial state and $P(\gamma_\tau, \tau|\gamma_0, 0)$ is the conditional probability that the internal angle has the value γ_τ at time τ when it is known to have the value γ_0 at time 0. If a priori probability $P(\gamma_0, 0)$ is assumed constant and the rotation about C-C bond is diffusional, it can be shown that the above ensemble average is reduced to the following form:

$$<\exp[i(m\gamma_0-m'\gamma_\tau)]> = \exp(-m^2 D\tau)\,\delta_{mm'} \tag{7}$$

where D is the diffusion coeffcient for rotation about a C-C bond. Thus we obtain from Eqs. (5) and (7)

$$G_N(\tau) = \sum_{a,b,\cdots,n} d_{ab}(\beta)^2 d_{ac}(\beta)^2\cdots d_{n0}(\beta')^2$$

$$+\exp[-(6D_0+a^2D_1+b^2D_2+\cdots+n^2D_N)\tau] \tag{8}$$

By making use of Eq. (8) we can write down the explicit form of $G_N(\tau)$ and T_1 for each carbon in a given n-alkane molecule. We present the formulas for T_1 derived under the extreme narrowing condition up to the sixth carbon in Appendix I.

London-Avitabile Model[3]. In this model the reorientation of C-H bonds is described as conformational finite jumps of $2\pi/3$ among three non-equivalent sites denoted by *trans*, gauche$^+$, and *gauche*$^-$ forms (see Figure 1) and the jump processes are treated on the basis of the first-order kinetics. Also, each conformational jump about any C-C bond is assumed independent of one another.

$$\underset{(g^+)}{\text{gauche}^+(\gamma=2\pi/3)} \rightleftarrows \underset{(t)}{\text{trans}(\gamma=0)} \rightleftarrows \underset{(g^-)}{\text{gauche}^-(\gamma=-2\pi/3)} \tag{9}$$

If we denote the mean lifetime for trans and gauche state, respectively, by τ_t and τ_g, the rate constant for jumping from the trans to gauche state and the inverse rate constant may be set equal to $1/2\tau_t$ and $1/\tau_g$, respectively. In this model

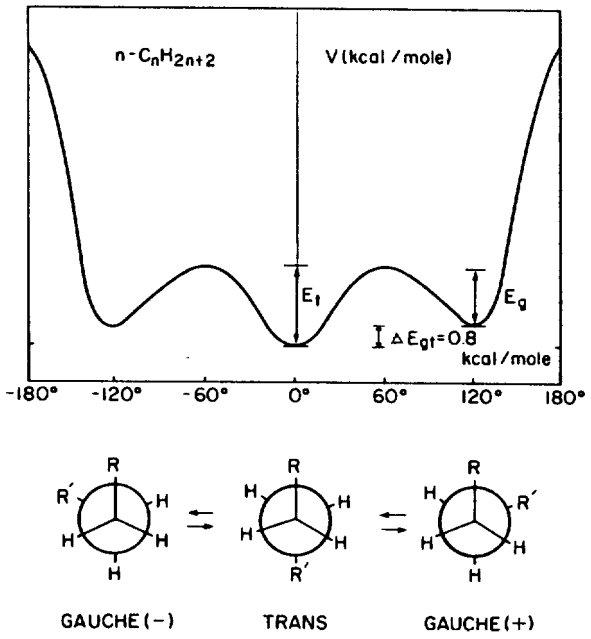

Figure 1. Conformational jumps and bond rotational potential energy in n-alkanes.

it is also assumed that direct jumps between gauche$^+$ and gauche$^-$ are forbidden because they are energetically unfavorable. In this case the expression of Eq. (6) should be replaced by

$$<\exp[i(m\gamma_0-m'\gamma_\tau)]>$$

$$=\sum_{\gamma_0=0,\,2\pi/3,\,-2\pi/3}\ \sum_{\gamma_\tau=0,\,2\pi/3,\,-2\pi/3} P(\gamma_0,\ 0)\, P(\gamma_\tau,\ \tau|\gamma_0,\ 0)$$

$$\times\exp[i(m\gamma_0-m'\gamma_\tau)] \tag{10}$$

From the rate equations for conformational interconversions shown in Eq. (11), London and Avitabile have derived the expressions for the conditional probabilities $P(\gamma_\tau, \tau|\gamma_0, 0)$ and utilized them to show that

$$<\exp[i(m\gamma_0-m'\gamma_\tau)]> = \frac{\sigma}{(1+2\sigma)^2}A_{mm'} \tag{11}$$

where σ is defined to be the relative probability of being in a gauche *vs.* trans state divided by 2; *viz.*,

$$\sigma=\frac{\tau_g}{2\tau_t}=\frac{[g^+]+[g^-]}{2[t]} \tag{12}$$

with $[t]$, $[g^+]$, and $[g^-]$, respectively, representing the equilibrium concentration of trans, gauche$^+$, and gauche$^-$ conformers. In the London-Avitabile model σ is assumed to be the same for all the C-C bonds.

The matrix A in Eq. (11) turned out to be a 5×5 matrix satisfying the following relations

$$A_{m,m'}=A_{m',m}=A_{-m,-m'}=A_{-m',-m}$$

and

$$A_{-2,-2}=A_{-1,-1}=A_{1,1}=A_{2,2}.$$

The expressions for the matrix elements A_{mn}'s are given in Appendix II.

Substitution of Eq. (11) into Eq. (5) leads to

$$G_N(\tau)=[\sigma/(1+2\sigma)^2]^N \exp(-6D_0\tau) \sum_{\substack{a,b,\cdots,n \\ b',c',\cdots,n'}} A_{aa} d_{ab} d_{ab'}\cdots$$

$$\times A_{nn'} d_{n0} d_{n'0} \exp[(-2\pi/3)i(n-n')] \quad (13)$$

The last exponential term on the righthand side of Eq. (13) is introduced due to the coordinates transformation from C-C bond to C-H bond. Taking the symmetry property of reduced Wigner matrix elements $d_{mm'}$ into account, the real part of $G_N(\tau)$ may finally be written as

$$G^N(\tau)=\left[\frac{\sigma}{(1+2\sigma)^2}\right]^N \exp(-6D_0\tau) \sum_{\substack{a,b,\cdots,n \\ b',\cdots,n'}}$$

$$\times[A_{aa} d_{ab} d_{ab'}][(-1)^{b+b'} A_{bb'} d_{bc} d_{b'c'}]\cdots$$

$$\times[(-1)^{m+m'} A_{mm'} d_{mn} d_{m'n'}][(-1)^{n+n'} A_{nn'} d_{n0} d_{n'0}]$$

$$\times\cos[(2\pi/3)(n-n')] \quad (14)$$

In Appendix III the explicit forms of $G_N(\tau)$ for this model are presented up to the sixth carbon in the chain. These $G_N(\tau)$'s are then Fourier-transformed to yield the relaxation time formulae. Thus the T_1 at the position of each carbon is found as a function of σ's and τ_i's for all the preceeding carbons and C-C bonds. In order to prevent the calculation from becoming unduly complicated we have introduced the following approximations:

(i) σ may be somewhat different for different C-C bond, but we assume it remains constant over the range of carbon chain investigated at a given temperature and depends only on temperature via the relation

$$\sigma=\exp(-\Delta E_{gt}/RT), \quad (15)$$

where ΔE_{gt} is the energy difference between trans and gauche state.

(ii) As a reasonable value for ΔE_{gt} we have taken 0.8 kcal/mole reported for *n*-butane.[17]

(iii) We also assume that the extreme narrowing approximation is valid for all the compounds investigated in this paper.

Experimentals

n-Octane through *n*-dodecane, all of spectroscopic grade, were purchased from Aldrich Chemical Co., Inc. The purity of these reagents were confirmed to be better than 99% by gas chromatography, but they were further purified by distillation under vacuum befor use. Four different solutions of 50, 20, 10, 5% (v/v) concentration in $CDCl_3$ were prepared for each compound and were put in 10 mm (O.D.) NMR tubes. These tubes were sealed under vacuum after they were degassed by repeating the standard freeze-pump-thaw cycle four times. T_1's have been measured for all of these samples to find the adequate concentration at which intermolecular effects are negligible. T_1 values found for 10 and 5% solutions were very close to each other and we have decided that at the concentration of 5% intermolecular effects are negligibly small. Thus all the T_1 data for ^{13}C reported in this paper are those for 5% solutions in $CDCl_3$ of the investigated compounds.

All the T_1 measurements were performed on a Varian VXR-200S NMR spectrometer operating at the field of 4.7

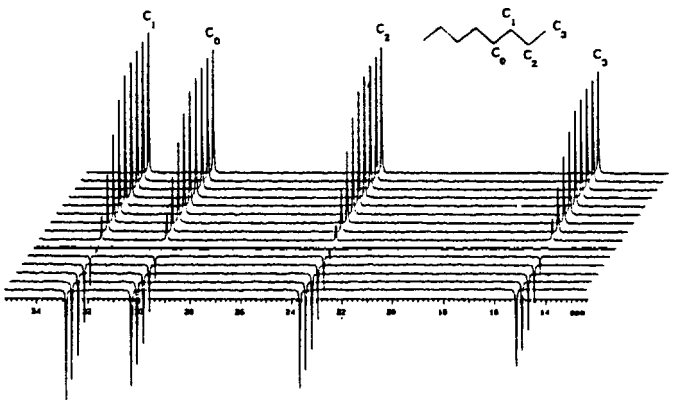

Figure 2. Stacked ^{13}C inversion recovery spectra under broadband proton decoupling for *n*-octane.

Table 1. Measured Relaxation Times T_1 for Carbon-13 and Effective Correlation Times in *n*-Octane

T (K)	^{13}C Relaxation Times, T_1 (sec)				Effective Correlation Times, τ_{eff} (10^{-12} sec)			
	C_0	C_1	C_2	C_3	C_0	C_1	C_2	C_3
248	4.14	4.47	4.90	6.24	5.94	5.50	5.02	3.94
258	4.77	5.11	5.57	7.28	5.16	4.81	4.42	3.38
268	5.54	5.91	6.40	8.23	4.44	4.16	3.84	2.99
278	6.16	6.70	7.22	9.10	3.99	3.67	3.41	2.70
288	6.64	7.27	7.93	10.38	3.70	3.38	3.10	2.37
298	7.62	8.30	9.17	11.90	3.23	2.96	2.68	2.07
308	8.49	9.23	10.27	13.50	2.90	2.67	2.40	1.82
318	9.42	10.22	12.43	15.23	2.61	2.41	1.98	1.61
Activation energy, E_a (Kcal/mol)					1.81	1.84	2.00	1.97

T under the condition of broadband proton decoupling by making use of the standard inversion recovery method. In order to enhance the signal sensitivity 20 or more FID's were collected for each measurement and to ensure the full recovery of equilibrium magnetization before applying a π pulse the delay time between two consecutive π-τ-$\pi/2$ pulse sequences was taken to be longer than five times the estimated T_1 value. The width for $\pi/2$ pulse used was 16.5 μsec. An illustrative example is shown in Figure 2. On the other hand, ^{13}C-{^1H} NOE factors[18] were evaluated *via* comparison of integrated intensities of spectral lines obtained under the condition of NOE enhancement and NOE suppression in the gated decoupling experiments and they were found to be nearly 2 for all the CH_2 carbons along the chain. The sample temperature was varied over the range of 238-318 K while being monitored with a calibrated copper-constantan thermocouple detector placed inside the probe to the accuracy fo ± 0.5℃. The chemical shift assignment for each ^{13}C signal was made on the basis of Grant-Paul rule[19] for linear alkane chains. All the T_1 data obtained at several different temperatures are listed in Table 1 through 5.

Calculation of Dynamic Parameters

Since the observed NOE factors are close to the theoretical

Table 2. Measured Relaxation Times T_1 for Carbon-13 and Effective Correlation Times in *n*-Nonane

T (K)	^{13}C Relaxation Times, T_1 (sec)					Effective Correlation Times, τ_{eff} (10^{-12} sec)				
	C_0	C_1	C_2	C_3	C_4	C_0	C_1	C_2	C_3	C_4
248	3.05	3.30	3.58	3.94	6.23	7.81	7.22	6.65	6.04	3.82
258	3.88	4.19	4.60	5.04	7.49	6.14	5.68	5.18	4.72	3.18
268	4.45	4.82	5.27	5.82	8.40	5.35	4.94	4.52	4.09	2.83
278	6.53	6.98	7.50	8.11	10.88	4.33	3.98	3.66	3.35	2.41
288	6.64	7.14	7.74	8.40	11.22	3.80	3.52	3.26	2.95	2.17
298	7.05	7.62	8.30	9.00	12.03	3.38	3.12	2.87	2.65	1.98
308	7.32	7.96	8.75	9.55	13.05	3.24	2.91	2.71	2.44	1.81
Activation energy, E_a (Kcal/mol)						2.29	2.32	2.30	2.29	1.88

Table 3. Measured Relaxation Times T_1 for Carbon-13 and Effective Correlation Times in *n*-Decane

T (K)	^{13}C Relaxation Times, T_1 (sec)					Effective Correlation Times, τ_{eff} (10^{-12} sec)				
	C_0	C_1	C_2	C_3	C_4	C_0	C_1	C_2	C_3	C_4
248	2.80	2.92	3.30	3.75	4.65	8.79	8.42	7.45	6.56	5.29
258	2.99	3.13	3.53	4.05	5.18	8.23	7.86	6.97	6.07	4.75
268	3.32	3.50	3.93	4.60	5.85	7.41	7.03	6.26	5.35	4.21
278	3.91	4.12	4.61	5.35	6.75	6.29	5.97	5.34	4.60	3.64
288	4.35	4.63	5.24	6.04	7.91	5.66	5.31	4.69	4.07	3.11
298	4.90	5.21	5.95	6.85	9.83	5.02	4.72	4.13	3.59	2.50
308	5.58	5.99	6.42	7.54	10.93	4.27	3.98	3.71	3.16	2.18
318	6.26	6.74	7.61	8.85	12.44	3.93	3.65	3.23	2.78	1.98
Activation energy, E_a (Kcal/mol)						1.89	1.96	1.93	1.91	2.32

maximum value for all the CH_2 carbons, we may conclude the dominant relaxation pathway is dipolar mechanism. Therefore we have calculated the effective correlation times, τ_{eff}'s for CH_2 carbons in the extreme narrowing limit from Eq. (16) and listed them in Tables 1 through 5.

$$\frac{1}{T_1} = \left(\frac{\mu_0}{4\pi}\right)^2 \frac{N_H \gamma_H^2 \gamma_C^2 \hbar^2}{r_{C-H}^6} \tau_{eff} = 2.15\times10^{10} N_H \tau_{eff} \quad (16)$$

Since τ_{eff} reflects the change of the orientation of C-H vector in the laboratory-fixed frame, it is expected to become shorter as we move away from the molecular center. Our results are in accord with this expectation. The Arrhenius-type plots of the observed τ_{eff}'s for C-H vectors in various *n*-alkanes are shown in Figure 3 through 7, which show the following relationship is valid:

$$\tau_{eff} = \tau_0 \exp(E_a/RT) \quad (17)$$

Although the mobility of a CH_2 group may be reflected

Table 4. Measured Relaxation Times T_1 for Carbon-13 and Effective Correlation Times in *n*-Undecane

T (K)	^{13}C Relaxation Times, T_1 (sec)						Effective Correlation Times, τ_{eff} (10^{-12} sec)					
	C_0	C_1	C_2	C_3	C_4	C_5	C_0	C_1	C_2	C_3	C_4	C_5
248	2.04	2.13	2.36	2.72	3.07	4.14	12.06	11.55	10.42	9.04	8.01	5.94
258	2.29	2.43	2.75	3.20	3.74	5.27	10.74	10.12	8.95	7.69	6.58	4.67
268	2.76	2.94	3.29	3.86	4.59	6.54	8.91	8.37	7.48	6.37	5.36	3.76
278	3.14	3.35	3.86	4.49	5.35	7.59	7.83	7.34	6.37	5.48	4.60	3.24
288	3.35	3.61	4.31	5.07	5.99	8.58	7.34	6.81	5.71	4.85	4.11	2.87
298	3.71	4.01	4.89	5.77	6.75	9.60	6.63	6.13	5.03	4.26	3.64	2.56
308	4.15	4.67	5.65	6.72	8.01	10.98	5.92	5.27	4.35	3.66	3.07	2.24
Activation energy, E_a (Kcal/mol)							1.79	1.94	2.20	2.26	2.35	2.40

Table 5. Measured Relaxation Times T_1 for Carbon-13 and Effective Correlation Times in *n*-Dodecane

T (K)	^{13}C Relaxation Times, T_1 (sec)						Effective Correlation Times, τ_{eff} (10^{-12} sec)					
	C_0	C_1	C_2	C_3	C_4	C_5	C_0	C_1	C_2	C_3	C_4	C_5
248	2.16	2.11	2.35	2.72	3.20	4.88	11.39	11.66	10.47	9.04	7.69	5.04
258	2.32	2.39	2.59	3.08	3.71	5.51	10.60	10.29	9.50	7.99	6.63	4.46
268	2.57	2.66	2.98	3.44	4.13	6.20	9.57	9.25	8.26	7.15	5.96	3.97
278	2.86	2.97	3.35	3.97	4.74	6.96	8.60	8.28	7.34	6.20	5.19	3.53
288	3.12	3.26	3.65	4.38	5.23	7.62	7.88	7.55	6.74	5.62	4.70	3.23
298	3.40	3.62	4.03	4.81	5.59	8.29	7.24	6.80	6.10	5.11	4.40	2.97
308	4.00	4.13	4.62	5.56	6.63	9.78	6.15	5.96	5.32	4.42	3.71	2.52
318	4.56	4.78	5.41	6.33	7.68	11.48	5.39	5.15	4.55	3.89	3.20	2.14
Activation energy, E_a (Kcal/mol)							1.64	1.76	1.81	1.86	1.87	1.82

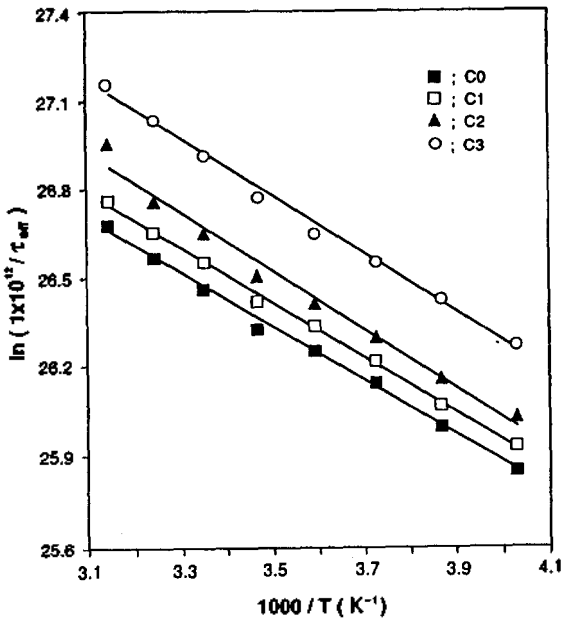

Figure 3. Plot of $\ln(1/\tau_{eff})$ *vs.* $1/T$ for *n*-octane.

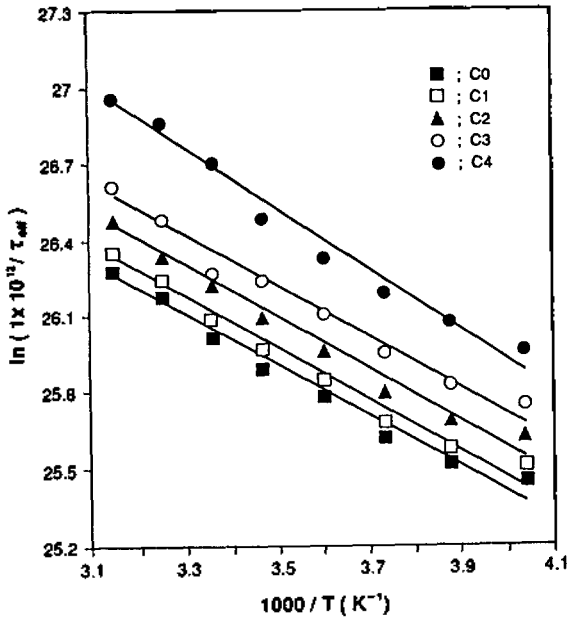

Figure 5. Plot of $\ln(1/\tau_{eff})$ *vs.* $1/T$ for *n*-decane.

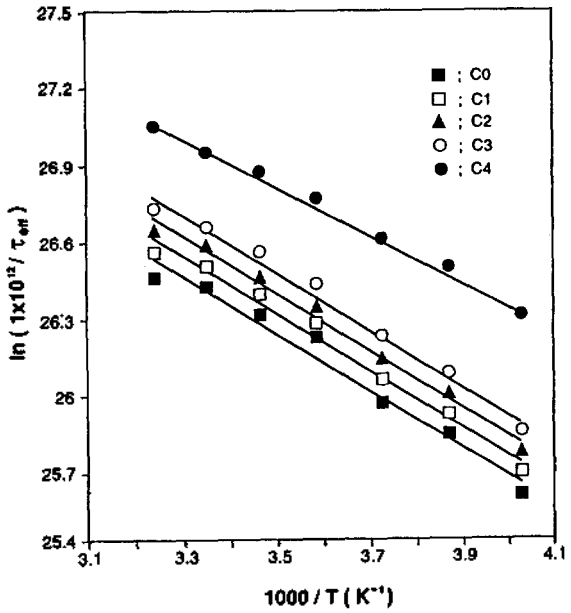

Figure 4. Plot of $\ln(1/\tau_{eff})$ *vs.* $1/T$ for *n*-nonane.

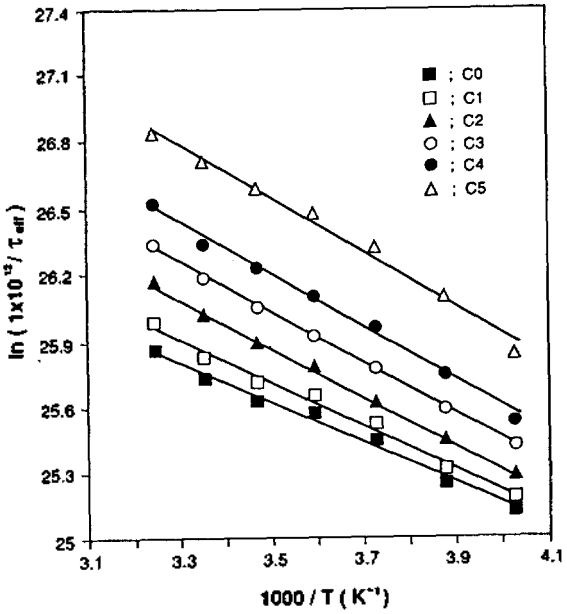

Figure 6. Plot of $\ln(1/\tau_{eff})$ *vs.* $1/T$ for *n*-undecane.

by τ_{eff}, we are more interested in the diffusion coefficients, D's, for the IRD model and the lifetimes of *trans* and *gauche* conformers, τ_t and τ_g, for the London-Avitabile model, since it is these quantities, rather than τ_{eff}, that correctly describe the relative motion of a CH_2 group with respect to neighboring inner CH_2's. D and τ_t for each C-C bond have been obtained by comparing measured T_1's with those calculated numerically from the expressions given in Appendix I, II and III under the extreme narrowing condition. Calculations have been made on an IBM 386 PC using the program written in the C and Pascal language and the results are shown in Table 6 through 10 and Figure 8 through 12. As we can see from these figures, the plot of $\ln(1/\tau_t)$ *vs* $(1/T)$ gives straight lines which means the following Arrhenius-type relation holds:

$$\frac{1}{2\tau_t} = A_t \exp\left(-\frac{E_t}{RT}\right) \tag{18}$$

where E_t is a measure of activation energy for the transition $t \rightarrow g$. Eq. (18) also gives the information about τ_g, when coupled with Eq. (5), from which one can calculate E_g, a measure of acivation energy for the transition $g \rightarrow t$. The difference between these two activation energies (ΔE_{gt}) is 0.80 kcal/mole as we have assumed at the outset of calculation. In contrast to this, the IRD model can yield only the information about the average activation energies E' through the

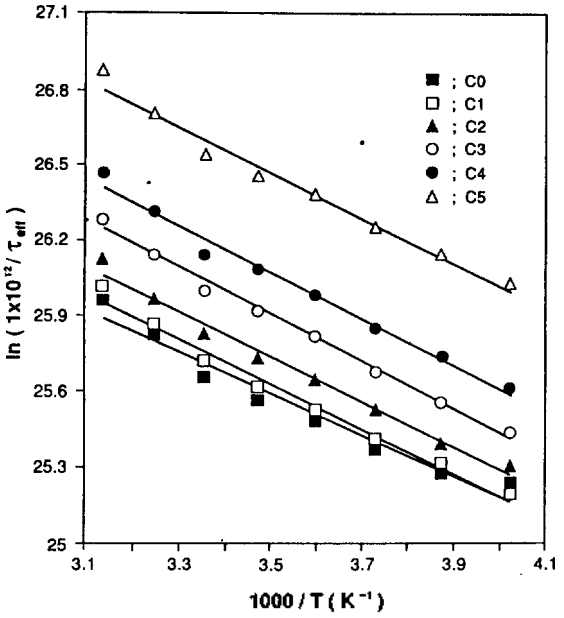

Figure 7. Plot of $\ln(1/\tau_{eff})$ *vs.* $1/T$ for *n*-dodecane.

Table 6. Rotational Diffusion Constants Calculated from the IRD Model and Mean Lifetimes for *trans*-Conformer Obtained from the L-A Model for *n*-Octane

T (K)	Rotational Diffusion Constants, D (10^9 see^{-1})			Life Times, τ_t (10^{-11} sec)		
	C_0-C_1	C_1-C_2	C_2-C_3	C_0-C_1	C_1-C_2	C_2-C_3
248	5.50	9.00	26.10	7.44	5.90	1.58
258	5.65	9.55	33.10	6.45	5.26	1.29
268	6.13	10.20	35.10	5.27	4.53	1.17
278	8.99	11.60	36.10	3.72	3.57	1.04
288	10.65	14.50	47.55	3.10	2.88	0.80
298	11.34	18.27	53.46	2.56	2.26	0.67
308	12.33	30.98	55.99	2.15	1.86	0.55
318	13.25	42.85	75.25	1.81	1.11	0.46
Activation energy (Kcal/mol)	E' 2.00	2.84	2.03	E_t 3.26	3.06	2.51

Table 7. Rotational Diffusion Constants Calculated from the IRD Model and Mean Lifetimes for *trans*-Conformer Obtained from the L-A Model for *n*-Nonane

T (K)	Rotational Diffusion Constants, D (10^9 see^{-1})				Life Times, τ_t (10^{-11} sec)			
	C_0-C_1	C_1-C_2	C_2-C_3	C_3-C_4	C_0-C_1	C_1-C_2	C_2-C_3	C_3-C_4
248	4.17	6.04	7.55	46.70	11.13	9.07	8.08	1.47
258	5.17	8.54	9.60	48.85	8.04	6.29	5.89	1.23
268	6.20	9.50	11.65	51.35	6.35	5.27	4.82	1.07
278	7.50	11.05	12.95	53.50	3.93	3.68	3.62	0.76
288	8.30	12.25	14.10	55.20	3.59	3.27	3.24	0.70
298	9.49	14.25	15.30	58.70	3.09	2.82	2.85	0.57
308	10.70	16.70	17.60	68.35	2.74	2.45	2.47	0.41
Activation energy (Kcal/mol)	E' 2.50	2.52	2.40	1.83	E_t 3.64	3.33	3.14	2.53

Table 8. Rotational Diffusion Constants Calculated from the IRD Model and Mean Lifetimes for *trans*-Conformer Obtained from the L-A Model for *n*-Decane

T (K)	Rotational Diffusion Constants, D (10^9 see^{-1})				Life Times, τ_t (10^{-11} sec)			
	C_0-C_1	C_1-C_2	C_2-C_3	C_3-C_4	C_0-C_1	C_1-C_2	C_2-C_3	C_3-C_4
248	1.98	7.09	9.70	18.12	20.00	9.81	7.69	2.60
258	2.31	7.55	11.00	22.75	16.94	8.90	6.79	2.17
268	2.96	8.25	13.80	25.75	13.09	7.65	5.50	1.85
278	3.50	9.40	15.30	28.70	10.18	6.31	4.71	1.58
288	4.65	11.85	16.95	39.80	7.64	4.85	3.90	1.21
298	5.15	14.25	19.35	60.69	6.37	3.95	3.27	0.79
308	6.79	15.24	22.61	66.98	4.68	3.20	2.63	0.62
318	7.97	17.35	25.90	73.10	3.78	2.78	2.27	0.46
Activation energy (Kcal/mol)	E' 3.13	2.18	2.14	3.46	E_t 3.89	3.02	2.79	2.45

Table 9. Rotational Diffusion Constants Calculated from the IRD Model and Mean Lifetimes for *trans*-Conformer Obtained from the L-A Model for *n*-Undecane

T (K)	Rotational Diffusion Constants, D (10^9 sec^{-1})					Life Times, τ_t (10^{-11} sec)				
	C_0-C_1	C_1-C_2	C_2-C_3	C_3-C_4	C_4-C_5	C_0-C_1	C_1-C_2	C_2-C_3	C_3-C_4	C_4-C_5
248	1.48	4.35	7.40	7.85	21.30	30.70	16.11	11.20	9.77	2.98
258	2.31	6.18	9.44	11.65	31.05	20.32	11.05	8.19	6.74	2.05
268	2.97	6.88	11.68	15.64	40.10	14.89	9.19	6.59	5.16	1.56
278	3.49	9.96	13.48	18.16	46.05	12.02	6.59	5.22	4.13	1.28
288	4.32	13.51	16.85	19.82	53.00	9.75	4.89	4.02	3.37	1.05
298	4.99	16.98	19.90	21.40	57.90	8.11	3.87	3.27	2.81	0.89
308	8.80	19.86	23.73	27.65	60.95	4.87	2.96	2.54	2.08	0.69
Activation energy E' (Kcal/mol)	3.88	4.18	2.90	3.00	3.04	E_t 3.83	3.72	3.67	3.23	3.01

Table 10. Rotational Diffusion Constants Calculated from the IRD Model and Mean Lifetimes for *trans*-Conformer Obtained from the L-A Model for *n*-Dodecane

T (K)	Rotational Diffusion Constants, D (10^9 sec^{-1})					Life Times, τ_t (10^{-11} sec)				
	C_0-C_1	C_1-C_2	C_2-C_3	C_3-C_4	C_4-C_5	C_0-C_1	C_1-C_2	C_2-C_3	C_3-C_4	C_4-C_5
248	0.83	4.32	7.62	10.24	34.50	44.08	17.58	11.53	8.78	2.19
258	1.16	3.75	9.55	13.55	37.45	32.08	17.88	9.81	7.03	1.91
268	1.47	5.90	9.60	14.30	42.85	25.12	11.87	8.41	6.14	1.64
278	1.81	7.05	12.75	16.60	45.90	19.88	9.66	6.44	4.96	1.42
288	2.31	7.33	14.76	18.61	49.35	15.68	8.66	5.56	4.31	1.27
298	3.65	8.10	15.70	17.50	55.40	10.77	7.13	4.86	4.06	1.13
308	1.95	9.10	19.10	23.45	65.50	12.45	6.72	4.23	3.21	0.89
318	4.65	11.85	19.20	28.35	79.20	8.16	4.79	3.59	2.55	0.64
Activation energy E' (Kcal/mol)	4.07	2.18	2.18	2.21	2.04	E_t 3.96	2.83	2.65	2.60	2.39

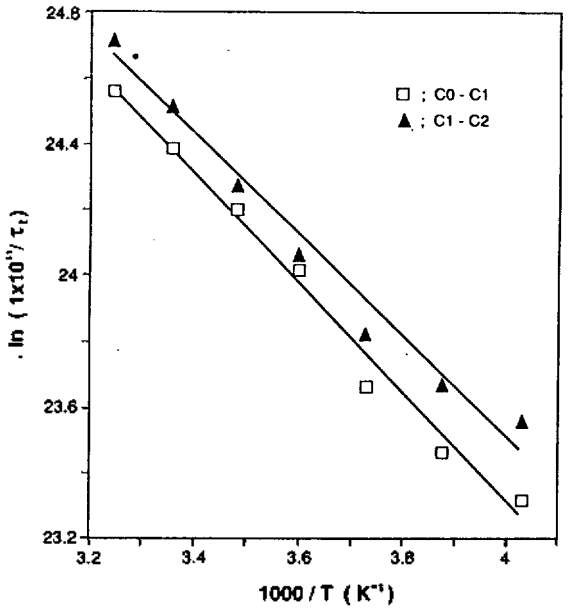

Figure 8. Plot of $\ln(1/\tau_t)$ *vs.* $1/T$ for *n*-octane.

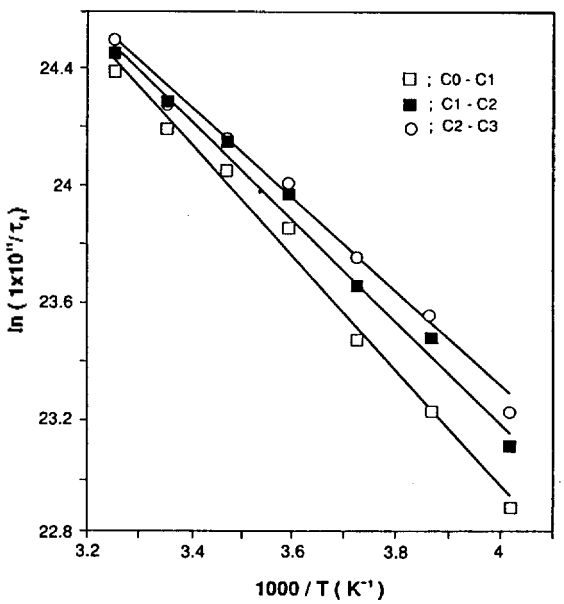

Figure 9. Plot of $\ln(1/\tau_t)$ *vs.* $1/T$ for *n*-nonane.

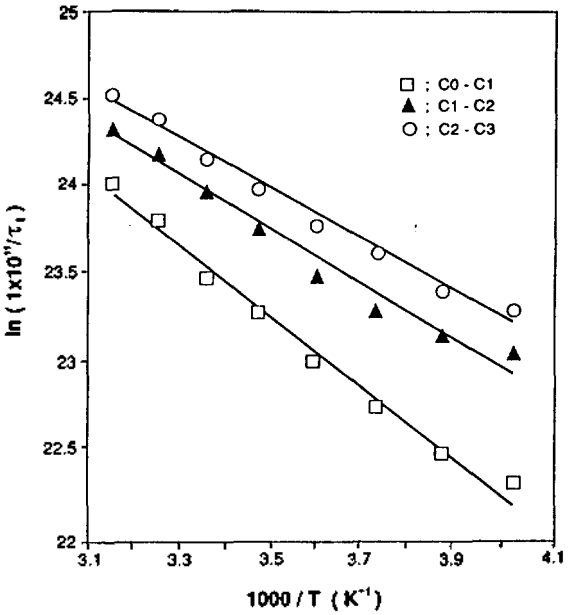

Figure 10. Plot of $\ln(1/\tau_i)$ *vs.* $1/T$ for *n*-decane.

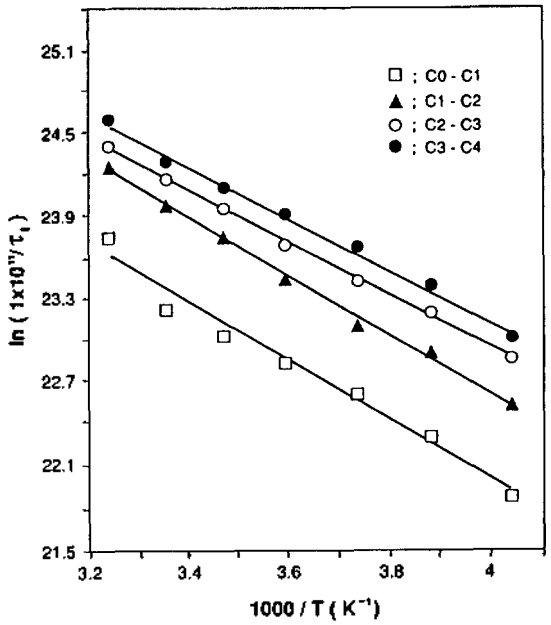

Figure 11. Plot of $\ln(1/\tau_i)$ *vs.* $1/T$ for *n*-undecane.

relation

$$D=D_0\exp\left(-\frac{E'}{RT}\right) \tag{19}$$

We have listed the values of E_t and E' obtained in this manner in Tables 6 through 10.

Results and Discussion

A quick look at Table 6 through 10 tells us that the barriers to rotation about C-C bonds are in the range of 2-4 kcal/mol, which approximately correspond to those associated to the internal rotation of a single bond in a small molecule, for all the compounds investigated in this work and slowly

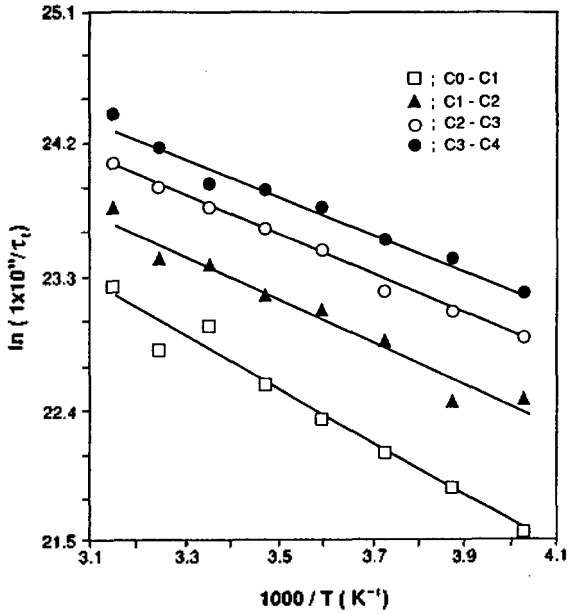

Figure 12. Plot of $\ln(1/\tau_i)$ *vs.* $1/T$ for *n*-dodecane.

increase as we move toward inner C-C bond along the chain. This is rather surprising, because much more rapid increase would be expected considering the effect of frictional force exerted by the solvent molecules. As Monnerie *et al.*[20] have pointed out, these low barrier heights and their gradual variation may be ascribed to the fact that actual rotations about C-C bonds proceed through the type 2 motions in Helfand's terminology, in which each rotation about a C-C bond is accompanied by β-coupled counter rotation(s) in neighboring C-C bonds. Earlier it has been asserted by Helfand[21] that this type of motion can appreciably reduce the frictional forces due to solvent molecules. Our observations are consistent with his assertion. Where it not for the segmental flexibilty of the chain, we would have much larger variation in barrier height. In predicting such trends, however, the IRD model does not seem to provide consistent results, as we can see from E' values listed in Tables 6 through 10, while the L-A model gives more satisfactory answers. This is not unusual considering that the IRD model is conceptually much cruder than the L-A model. Thus one may say that the IRD model is too crude to be used for the study of segmental motions even for such short chain compounds as *n*-alkanes ranging from octane to dodecane. The L-A model provides a simple way to correlate the barrier height to rotation about C-C bonds with observed NMR relaxation data, but its great weakness lies in the fact that it does not explicitly take the correlations among rotations about different C-C bonds into formulation. But it does not disregard such correlations either. In fact a $t\rightarrow g$ transition may involve many different correlated rotations, such as $ttt\rightarrow g^+tg^-$, $ttg\rightarrow gtt$, *etc.* Thus the barrier height to rotation about a given C-C bond inferred from the L-A model may be considered as a sort of average value taken over these various concerted rotations. In other words one simply cannot tell how much each type of motion will contribute to the modulation of orientation of C-H internuclear vector on the basis of the L-A model. It will be difficult to incorporate the idea of concerted (or

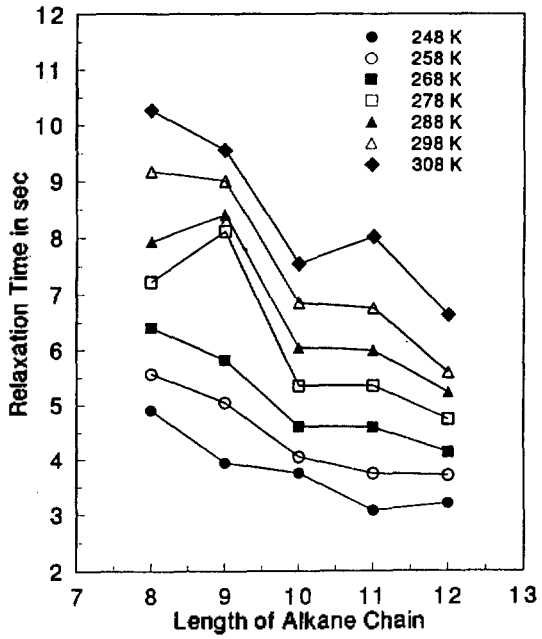

Figure 13. Even-odd alternation of T_1 for methylene carbon next to methyl group at various temperatures (All other carbons were found to behave similarly, though not shown here).

correlated) rotations into the original L-A theory without modifying the model itself in such a way that it explicitly takes these types of motion into consideration from the outset. In order to gain further insights into these questions we will have to resort to a more detailed theoretical mode, which is under investigation in our research group. Nevertheless, the information obtained from the L-A model provides us at least semi-quantitative knowledge of the motional type and the barrier height in the investigated compounds.

Activation energies calculated directly from τ_{eff} of carbons [see Table 1 through 5] are smaller than E_t's, which means overall rotation still plays important roles in dynamics of the molecules investigated in this work. We believe the reason for this is two fold. First the chains of our molecules are open at both ends and are not long enough compared to ordinary polymeric chain. Secondly, the solvent used in our experiment, $CDCl_3$, is not viscous enought to retard the overall rotation. Use of longer chain compounds and more viscous solvents will shed more light on this question.

One more noteworthy thing is that, when plotted against the chain length, T_1 value for a given carbon shows zig-zag shaped variation (see Figure 13), depending on whether the number of carbons in the chain is even or odd. Such phenomenon has already been known for alkane chains in solid state,[22] but we are somewhat amazed that it can still be observed even for dissolved state. This, we believe, has something to do with the type 2 motions in which even numbers of rotation are always involved. Further investigation is under way in our laboratory.

Acknowledgement. This work was supported by a grant (Project No. ED 89-30) from the Basic Science Research Institute Program, Ministry of Education, Korea, 1989.

References

1. J. Skolnick and E. Helfand, *J. Chem. Phys.*, **72**, 5489 (1980).
2. J. Skolnick and E. Helfand, *J. Chem. Phys.*, **77**, 5714 (1982).
3. R. E. London and J. Avitabile, *J. Am. Chem. Soc.*, **99**, 7765 (1977).
4. J. Luque, J. Santamaria, and J. J. Freire, *J. Chem. Phys.*, **91**, 584 (1989).
5. J. P. Ryckaert, *Mol. Phys.*, **55**, 549 (1985).
6. R. M. Levy, M. Karplus, and P. G. Wolynes, *J. Am. Chem. Soc.*, **103**, 5998 (1981).
7. M. Fixman, *Faraday Discuss. Chem. Soc.*, **83**, 119 (1987).
8. S. Karaborni and I. P. O'Connel, *J. Chem. Phys.*, **92**, 6190 (1990).
9. D. Wallach, *J. Chem. Phys.*, **47**, 5258 (1967).
10. F. Geny and L. Monnerie, (a) *J. Polym. Sci., Polym. Phys. Ed.*, **17**, 131 (1979); (b) *ibid*, 17, 147 (1979).
11. F. Geny and L. Monnerie, *J. Chem. Phys.*, **66**, 1691 (1969).
12. A. P. Marchand, *Application of NMR Spectroscopy to Problems in Stereochemistry and Conformational Analysis*, chap. 3, VCH Pub. Inc., 1986.
13. Y. K. Levine, N. Birdsall, A. G. Lee, J. C. Metcalfe, P. Partington, and G. C. K. Roberts, *J. Chem. Phys.*, **60**, 2890 (1974).
14. H. Versmold, *J. Chem. Phys.*, **58**, 5649 (1973).
15. R. J. Witterbort and A. Szabo, *J. Chem. Phys.*, **69**, 1722 (1978).
16. T. E. Bull, *Chem. Phys.*, **121**, 1 (1988).
17. G. Govil, R. V. Hosur, *Conformation of Biological Molecules*, pp. 4-7, Springer-Verlag, NY (1982).
18. An NOE factor is defined as $(I/I_0)-1$, where I and I_0 are NOE enhanced and NOE suppressed signal intensity, respectively.
19. D. M. Grant and E. G. Paul, *J. Am. Chem. Soc.*, **86**, 2984 (1964).
20. L. Monnerie and F. Laupretre, *Spcetroscopic Investigation of Local Motions in Polymers* in *Structure and Dynamics of Molecular Systems*−II (ed. Daudel, *et al.*, Reidel Pub. Co., 1986), pp. 129-154.
21. E. Helfand, Science, **226**, 647 (1984).
22. M. Okazaki and K. Toriyama, *J. Phys. Chem.*, **93**, 2883 (1989).

Appendix I

$$C_0(\text{first carbon}) : \frac{1}{T_1} = 20\ K \cdot \frac{1}{6D_0}$$

$$C_1(\text{second carbon}) : \frac{1}{T_1} = 20K \sum_{a=-2}^{2} (d_{a0})^2 \frac{1}{6D_0 + a^2D_1}$$

$$C_2(\text{third carbon}) : \frac{1}{T_1} = 20K \sum_{a,b} (d_{ab})^2 (d_{b0})^2 \times \frac{1}{6D_0 + a^2D_1 + b^2D_2}$$

$$C_3(\text{fourth carbon}) : \frac{1}{T_1} = 20K \sum_{a,b,c} (d_{ab})^2 (d_{bc})^2 (d_{c0})^2 \times \frac{1}{6D_0 + a^2D_1 + b^2D_2 + c^2D_3}$$

$$C_4(\text{fifth carbon}) : \frac{1}{T_1} = 20K \sum_{a,b,c,d} (d_{ab})^2 (d_{bc})^2 (d_{cd})^2 (d_{d0})^2$$

$$\times \frac{1}{6D_0+a^2D_1+b^2D_2+c^2D_3+d^2D_4}$$

$$C_5(\text{sixth carbon}) \therefore \frac{1}{T_1} = 20K \sum_{a,b,c,d,e} (d_{ab})^2(d_{bc})^2(d_{cd})^2(d_{de})^2(d_{e0})^2 \times \frac{1}{6D_0+a^2D_1+b^2D_2+c^2D_3+d^2D_4+e^2D_5}$$

where $K=(N_H/10)(2\pi R)^2=2.15\times10^9$ N_H

Appendix II

$A_{00}=(1+2\sigma)^2/\sigma$

$A_{20}=A_{10}=A_{02}=A_{01}$
$=A_{-20}=A_{-10}=A_{0-2}=A_{0-1}$
$=(1/\sigma)-2\sigma+1$

$A_{11}=A_{-1-1}=A_{22}=A_{-2-2}$
$=A_{-12}=A_{2-1}=A_{-21}=A_{1-2}$
$=(1/\sigma)+\sigma-2+(9/2)\ \exp(-\tau/\tau_g)$
$+(3/2)(1+2\sigma)\ \exp(-\tau/\tau_g)$

$A_{1-1}=A_{-11}=A_{12}=A_{21}$
$=A_{2-2}=A_{-22}=A_{-1-2}=A_{-2-1}$
$=(1/\sigma)+\sigma-2+(9/2)\ \exp(-\tau/\tau_g)$
$-(3/2)(1+2\sigma)\ \exp(-\tau/\tau_g)$

where $1/\tau_g=1/\tau_t+1/\tau_g$

Appendix III

$G_0(\tau_g)=\exp\ (-6D_0\tau)$

$G_1(\tau_g)=[\sigma/(1+2\sigma)^2]\ \exp(-6D_{0\tau})\ \sum_{a=-2}^{2} d_{a0}\,d_{a0}\,A_{aa}$

$G_2(\tau_g)=[\sigma/(1+2\sigma)^2]^2\ \exp(-6D_{0\tau})$
$\times\sum_{a}\sum_{bb'} d_{ab}\,d_{ab'}\,d_{b0}\,d_{b'0}\,A_{aa}\,A_{bb'}\ \cos[(2\pi/3)(b-b')]$

$G_3(\tau_g)=[\sigma/(1+2\sigma)^2]^3\ \exp(-6D_{0\tau})$
$\times\sum\sum\sum d_{ab}\,d_{ab'}\,d_{bc}\,d_{b'c'}\,d_{c0}\,d_{c'0}\,A_{aa}\,A_{bb'}\,A_{cc'}$
$\times\cos[(2\pi/3)(c-c')]$

$G_4(\tau_g)=[\sigma/(1+\sigma)^2]^4\ \exp(-6D_{0\tau})$
$\times\sum_{a}\sum_{bb'}\sum_{cc'}\sum_{dd'} d_{ab}\,d_{ab'}\,d_{bc}\,d_{b'c'}\,d_{cd}\,d_{c'd'}$
$\times d_{d0}\,d_{d'0}\,A_{aa}\,A_{bb'}\,A_{cc'}A_{dd'}\ \cos[(2\pi/3)(d-d')]$

$G_5(\tau_g)=[\sigma/(1+2\sigma)^2]^5\ \exp(-6D_{0\tau})$
$\times\sum_{a}\sum_{bb'}\sum_{cc'}\sum_{dd'}\sum_{ee'} d_{ab}\,d_{ab'}\,d_{bc}\,d_{b'c'}\,d_{cd}\,d_{c'd'}$
$\times d_{de}\,d_{d'e'}\,d_{e0}\,d_{e'0}\,A_{aa}\,A_{bb'}\,A_{cc'}\,A_{dd'}\,A_{ee'}$
$\times\cos[(2\pi/3)(e-e')]$

Influence of Ammonia Solvation on the Structural Stability of Ethylene Cluster Ions

Kwang Woo Jung, Sung-Seen Choi, and Kyung-Hoon Jung*

Center for Molecular Science and Department of Chemistry
Korea Advanced Institute of Science and Technology, Taejon 305-701

Du-Jeon Hang

Department of Chemistry, Seoul National University, Seoul 151-742
Received January 27, 1992

The stable structures of pure ethylene and mixed ethylene-ammonia cluster ions are studied using an electron impact ionization time-of-flight mass spectrometer. Investigations on the relative cluster ion distributions of $(C_2H_4)_n(NH_3)_m^+$ under various experimental conditions suggest that $(C_2H_4)_2(NH_3)_3^+$ and $(C_2H_4)_3(NH_3)_2^+$ ions have the enhanced structural stabilities, which give insight into the feasible structure of solvated ions. For the stable configurations of these ionic species, we report an experimental evidence that both $(C_2H_4)_2^+$ $(C_2H_4)_3^+$ clusters as the central cations provide three and two hydrogen-bonding sites, respectively, for the surrounding NH_3 molecules. This interpretation is based on the structural stability for ethylene clusters and the intracluster ion-molecular rearrangement of the complex ion under the presence of ammonia solvent molecules.

Introduction

The most remarkable progress in the cluster ion chemistry is the recent finding of the intracluster ion-molecule reactions.[1-4] As a large number of neutral molecules attach to the central ion, the gas phase becomes to resemble that pertaining in solution in the vicinity of ions. The careful study of this system, thus, makes it possible to bridge the gap between gas-phase and solution chemistry. This in turn permits a more precise understanding of the nature of solution of ions by solvent molecules.[5]

Numerous experimental attentions[6,7] have been also paid

*Author to whom correspondence should be addressed.